Flexible Sensor Film Based on Rod-Shaped SWCNT-Polypyrrole Nanocomposite for Acetone Gas Detection

Hyo-Kyung Kang , Jun-Ho Byeon , Hun-Jun Hwang , Yoon Hee Jang * , Jin-Yeol Kim *

Posted Date: 7 July 2023

doi: 10.20944/preprints202307.0467.v1

Keywords: Flexible gas sensor, SWCNT-PPy composite, Acetone gas sensor, Polyimide substrate, Room temperature

Article

Flexible sensor Film Based on Rod-Shaped SWCNT-Polypyrrole Nanocomposite for Acetone Gas Detection

Hyo-Kyung Kang [1] Jun-Ho Byeon [1] Hyun-Jun Hwang [1] Yoon Hee Jang [2]* and Jin-Yeol Kim [1]*

[1] School of Advanced Materials Engineering, Kookmin University, Seoul 02707, Korea
[2] Advanced Photovoltaics Research Center, KIST, Seoul 02792, Korea
* Correspondence: Correspondence: yhjang@kist.re.kr; jinyeol@kookmin.ac.kr

Abstract: A nanocomposite rod-shaped structure with single-walled carbon nanotube (SWCNT) embedded in polypyrrole (PPy) doped with nonafluorobutanesulfonic acid (C4F), SWCNT/C4F-PPy, was synthesized using emulsion polymerization. The hybrid ink was then directly coated on a polyimide film interdigitated with the Cu/Ni/Au electrodes via a screen-printing technique to create a flexible film sensor. The sensor film showed a response of 1.72% at 25 °C/atmospheric pressure when acetone gas of 5 ppm was injected, which corresponds to almost 95% compared to the Si wafer-based array interdigitated with the Au electrode. Additionally, C4F was used as a hydrophobic dopant of PPy to improve the stability of humidity and to produce a highly sensitive film-type gas sensor that provides stable detection even in humid conditions.

Keywords: flexible gas sensor; SWCNT-PPy composite; acetone gas sensor; polyimide substrate; room temperature

1. Introduction

Gas detectors have been a subject of great interest over the past few decades in response to industrial and medical demands in air quality monitoring [1], the automotive [2] and semiconductor industries, and in the screening or monitoring of various diseases [3,4]. Basically, a gas sensor consists of a passivation layer between a gas-sensing layer and a substrate interdigitated with electrodes. Most gas sensor substrates consist of alumina plates [5], ceramic plates [6], or silicon wafers [7], and the gas-sensing layers consist of metal oxides [8–10], such as ZnO [8], In_2O_3 [9], SnO_2 [10], and WO_3 [11]. Recently, flexible gas sensors [12–17] based on plastic substrates, such as polyimide (PI) [12,13], polycarbonate (PC) [14], and polyethylene terephthalate (PET) [15,16] films have been developed to achieve lower manufacturing costs as well as improved miniaturization, portability, and wearability. In addition, gas sensors that use π-conjugated carbon compounds (CCC), such as carbon nanotube (CNT) [17–19], polypyrrole (PPy) [13,20–22], polyaniline (PANi) [16,23], and graphite [24] as a gas-sensing layer are being actively studied. These CCC-based sensors exhibit improved features for gas detection [13,16–24]. They operate at low temperatures and the sensing material can be designed to detect selected compounds with very low-response to other compounds. Furthermore, they can be processed into thin films using a screen-printing process. Kumar et al [16]. described an ammonia gas sensor based on PANi as a gas-sensing layer deposited on a PET film and investigated the ammonia gas-sensing properties of the film at 25℃ from 5–1000 ppm. Hua et al [19]. reported a potential gas sensor for NH_3, NO, and NO_2 sensing applications using a single-walled CNT–Fe_2O_3 (SWCNT-Fe_2O_3) composite film deposited on a PI film substrate. Additional research into the potential applications of flexible gas sensors is ongoing, and new manufacturing technologies, such as screen printing and flexible film-forming processes are critical to produce low-cost efficient sensors.

In this work, we first fabricated an interdigitated electrode (IDE) with a Cu/Ni/Au three-layer structure on a flexible 50 μm-thick PI film (IDE PI film). Second, a film-type flexible gas sensor was fabricated using a nonafluorobutanesulfonic acid-doped-polypyrrole (C4F-PPy) and SWCNT

Preprints (www.preprints.org) | NOT PEER-REVIEWED | Posted: 7 July 2023 doi:10.20944/preprints202307.0467.v1

nanocomposite ink, i.e., SWCNT/C4F-PPy, on an IDE PI film by screen printing to detect acetone gas. Figure 1 depicts the schematic diagram of a flexible gas sensor film with gas-sensing layers on an IDE PI substrate. Screen printing is advantageous due to its low cost, high-speed patterning, and applicability to various substrates, making it an efficient alternative to conversion patterning techniques used in the production of multi-purpose electronic devices. Particularly, screen-printed sensor films can offer more benefits in terms of mass production, control of sensing dimensions, and flexibility. The SWCNT/C4F-PPy nanocomposite sensor film was able to detect less than 1 ppm of acetone gas at 25℃ and exhibited moisture-resistance. The film sensors demonstrated a response of 1.72% at 5 ppm acetone concentration, which corresponds to nearly 95% of the sensor response of the Si wafer substrate with integrated Au electrodes, providing promise of good response characteristic at high humidity concentrations.

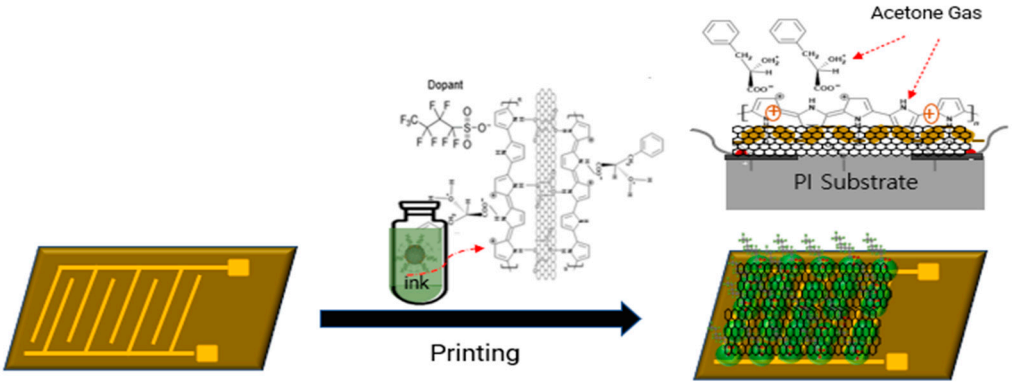

Figure 1. Top-view and cross-section schematic diagram of a flexible sensor film with SWCNT/C4F-PPy nanocomposite layers on an IDE polyimide substrate (left; IDE substrate, right; flexible gas sensor film). IDE substrate consists of two contact pads (2 mm × 2.5 mm) and a sensor electrode (width: 0.5 mm, distance: 0.8 mm) composed of the Cu/Ni/Au three-layers. The sensor area is 8 mm × 10 mm. The sensor film on the right shows the layers composed of a rod-shaped SWCNT/C4F-PPy nanostructure.

2. Materials and Methods

2-1. Fabrication of PI film interdigitated with Cu/Ni/Au electrodes: IDE substrate

The fabrication process of the IDE substrate is shown in Figure 2. It was designed based on a 50-μm-thick flexible PI film (Kapton, Dupont, USA), where the electrode geometry is set to a level that enables higher sensor responsibility. First, the flexible PI film and 6-μm-thick Cu foil, which is treated with hot melt adhesive, were bonded by a hot lamination process at 200 °C. Then the Cu-laminated PI film was patterned via a photolithography process, and finally, a 2– 3-μm Ni and Au layers were sequentially formed on the Cu layer using electroless plating. The result was an IDE substrate film consisting of two contact pads (2 mm × 2.5 mm) and a sensor electrode (width: 0.5 mm, distance: 0.8 mm) composed of a Cu/Ni/Au three-layered-metal. Here, Au in the surface layer of the 3-layered electrode was configured to prevent oxidation and improve electrical conductivity, thereby providing an electrical resistance of 0.1Ω•cm. Then, the as-prepared IDE substrate film was pre-treated with polycationic poly (dimethyl-diallyl ammonium chloride) (PDDA, Sigma-Aldrich) aqueous solution (1%) and a polyanionic poly (sodium 4-styrenesulfonate) (PSS, Sigma-Aldrich) aqueous solution (2 mg/ml; pH ≈ 1 adjustment) was sequentially applied using a layer-by-layer technique to get a negatively charged surface layer as shown in Figure 2.

Preprints (www.preprints.org) | NOT PEER-REVIEWED | Posted: 7 July 2023 doi:10.20944/preprints202307.0467.v1

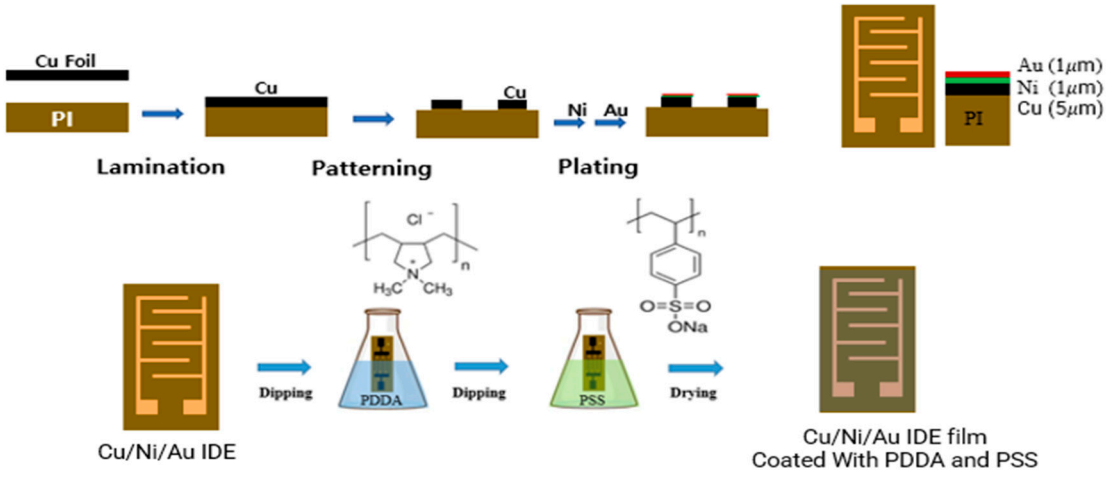

Figure 2. Schematic showing the preparation of the PI substrates interdigitated with the Cu/Ni/Au electrodes (IDE substrate). The IDE electrode lines have a distance and width of 0.8 mm and 0.5 mm, respectively. The PI substrate used has 50 μm-thick film. The prepared IDE substrate film was treated with PDDA and PSS via a layer-by-layer technique to obtain a negatively charged surface layer, which improves the adhesion properties between the sensing material and the upper layer.

2.-2. Synthesis of SWCNT/C4F-PPy nanocomposite

The rod-shaped SWCNT/C4F-PPy nanocomposite was synthesized using an emulsion polymerization technique described in a previous paper [22]. The synthesized proceeded in five steps. First, hydroxypropyl methylcellulose (HPMC, Sigma-Aldrich) was dissolved in deionized (DI) water to prepare 1wt% dispersion solution. Then, 0.0031 g of SWCNTs (Zeon, Japan) was added to a 30 mL of HPMC solution and sonicated for 30 min. Second, 0.3 g of pyrrole monomer and 0.37 g of L-(-)-3-Phenyllactic Acid (PLA) were each dissolved in a 30 mL of HPMC and SWCNT mixed solutions in order and stirred at 0 ℃ for 30 min. Forth, 3.11 g of iron chloride hexahydrate ($FeCl_3 \bullet 6H_2O$), as an oxidant, was added to the mixture, and reacted at 0 °C for 6 h to complete the synthesis of the final solution. Finally, 560ul of C4F (40wt% aqueous solution) (pyrrole:C4F = 1:0.1 molar ratio) was added as a dopant and the mixture was stirred for more than 12 h. Scheme 1 provides a representation of the synthesized rod-shaped SWCNT/C4F-PPy nanostructures. The synthesized nanostructure was purified 2 to 3 times using ultracentrifugation. The synthesized rod-shaped SWCNT/C4F-PPy nanocomposite (3wt%) was prepared as an ink redispersed in a mixed solvent of DI water–isopropanol (1:1 v/v) with 2wt% HPMC.

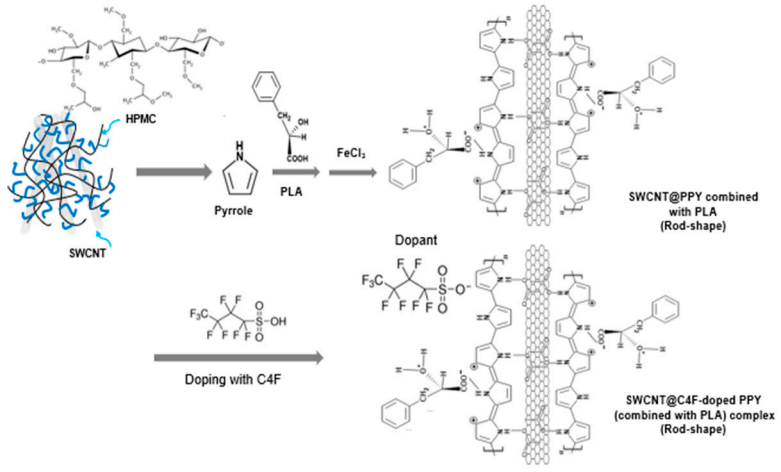

Scheme 1. The synthetic procedure for the fabrication of a water-dispersible rod-shaped SWCNT/C4F-PPy nanostructure. .

 doi:10.20944/preprints202307.0467.v1

2.-3. Performance evaluation of gas sensors

The ink solutions using the as-synthesized SWCNT/C4F-PPy nanocomposite were coated on the prepared IDE substrate strip through screen printing technology to form a sensing layer, and then dried in a vacuum oven at 60°C for 1 hour. The prepared sensor strip (test cell) was installed in the test chamber and the resistance value changed according to gas injection was measured using an electrochemical detection method. Pure dry air was injected as the carrier gas for 10 min while maintaining the chamber pressure at atmospheric pressure. Then, C_3H_6O gas was exposed to concentration of 2.5 and 5 ppm at 25°C, in dry air (0% relative humidity (RH)) and wet conditions (10 to 80%RH/25°C). The resistances between electrodes were measured under the constant DC applied current. The resistances between electrodes were measured under a constant DC applied current. The current resistance (Ω, ohm) was measured using a resister (Keithley 2000) by applying a DC voltage of 2 V.

3. Results and Discussion

The overall synthetic procedure used to create the water-dispersible SWCNT/C4F-PPy nanocomposite is described in Scheme 1. First, an aqueous HPMC solution where SWCNTs were uniformly dispersed was prepared for emulsion polymerization and then pyrrole monomer and PLA were sequentially added to it. $FeCl_3$ was then added as an oxidizing agent to initiate the polymerization reaction. This resulted in the formation of a rod-shaped nanostructure with SWCNT at the core surrounded by PPy–PLA (Scheme 1). A previous study reported that PLA is chemically bonded with the PPy chain and reacts selectively with a specific gas such as acetone [22]. The resulting products can maintain long-term dispersion stability in aqueous solution without precipitation due to its excellent dispersion characteristics. Structurally, SWCNTs surface-treated with COOH are chemically interconnected with NH groups of the pyrrole ring and can also electrically transfer electrons. SWCNTs with high electrical conductivity can greatly increase electrical conductivity by extending the electron transport path with PPy, which is an electrically conductive polymer chain. Notably, SWCNTs have been shown to improve the electrical conductivity of PPy by more than 30%. A resistance value of 24 KΩ•cm was measured on a 10-μm-thick SWCNT/C4F-PPy film. For screen printing, the synthesized SWCNT/C4F-PPy nanocomposite (3wt%) was redispersed in a mixed solvent of DI water–isopropanol (1:1 v/v), where 2wt% HPMC was dissolved to prepare a coating ink.

The SEM and TEM images (Figure 3 (I) and (II)) of the SWCNT/C4F-PPy nanostructures printed on the PI film of the as-prepared IDE pattern show that the SWCNT/C4F-PPy has rod-like nanostructures (approximately 60-nm-diameter and 3-μm-length). In particular, the SWCNT/C4F-PPy nanostructures have a core–shell structure surrounded by a C4F-doped-PPy layer with a thickness of approximately 30 nm on the outer surface of the SWCNT single strand. Figure 3 (III) displays energy dispersive X-ray spectroscopy (EDS) spectral data, which was used for component analysis of SWCNT/C4F-PPy. The analysis showed that the contents of major atoms such as C, O, N, S, and F were 62.24%, 6.01%, 14.09%, 0.93%, and 1.15%, respectively. Notably, EDS data confirmed the presence of S and F atoms present in the C4F molecule, which is used as the dopant. C4F containing fluorine (F) is used as a hydrophobic dopant for π-conjugated polymer, PPy, to improve resistance to external humidity and to control the electrical conductivity of PPy.

Preprints (www.preprints.org) | NOT PEER-REVIEWED | Posted: 7 July 2023 doi:10.20944/preprints202307.0467.v1

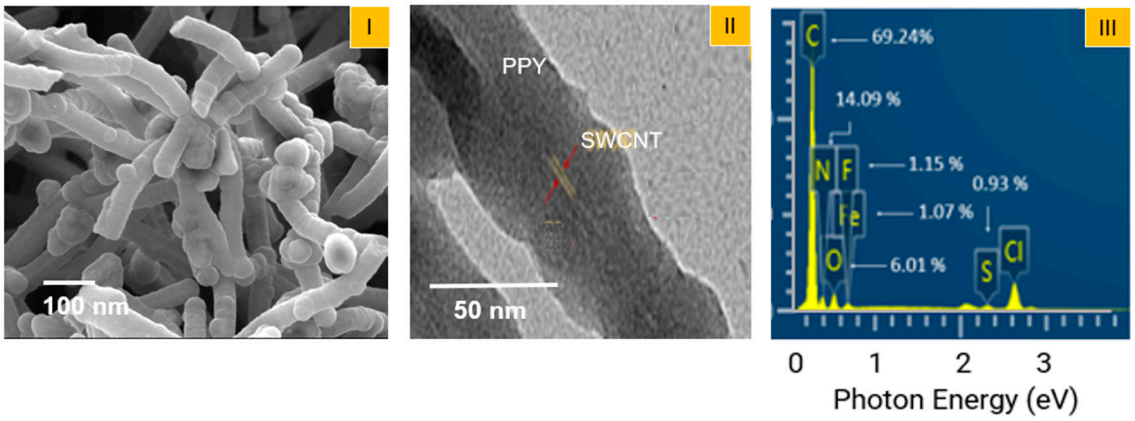

Figure 3. (I) SEM and (II) TEM morphologies of SWCNT/C4F-PPy core–shell shaped nanorods. (III) EDS spectra showing the elemental analysis data for SWCNT/C4F-PPy.

Externally humidity plays an important role in the stability and performance of biosensors. Therefore, obtaining a reliable response to humidity in biosensors and avoiding cross-response due to moisture remains a major challenge [25]. As is widely known, most organic-based sensors including metal oxide sensors exhibit lower response under humid conditions. Herein, we synthesized a hydrophobic PPy nanocomposite, SWCNT/C4F-PPy nanocomposites, using C4F as a dopant to ensure the stability of the sensor material in humid conditions. Previous researchers [26] studied the stability of a PPY-based acetone gas sensor in humid conditions using C8F as a dopant, and based on their results, we believed that C4F would also make the PPy surface hydrophobic and neutralize it, implying that C4F can be used to impart materials with water-repellent properties. Figure 4 shows the change in electrical resistance of the SWCNT/C4F-PPy films as a function of relative humidity (RH). As shown in Figure 4-I(a), the control of SWCNT/PPy film (no C4F) exhibited a significant change in resistance with an increase in the RH% at 25 °C. In contrast, resistance was rapidly stabilized as the C4F content increased to 0.05, 0.1, 0.2, and 0.3 molar ratio based on the pyrrole monomer (Figure 4-I(b), (c), (d), and (e)). Humidity stability was also improved when the C4F content was 0.1 mol/ratio or more; however, the response of the sensor was rapidly decreased. Figure 4-(II) shows the humidity stability of the SWCNT/C4F-Ppy (C4F content: 0.1 molar ratio) film at three different temperatures. In particular, humidity stability was doubled when the temperature was 40 ~55 ℃, and was improved by 1.5 times at 60 ~90 ℃.

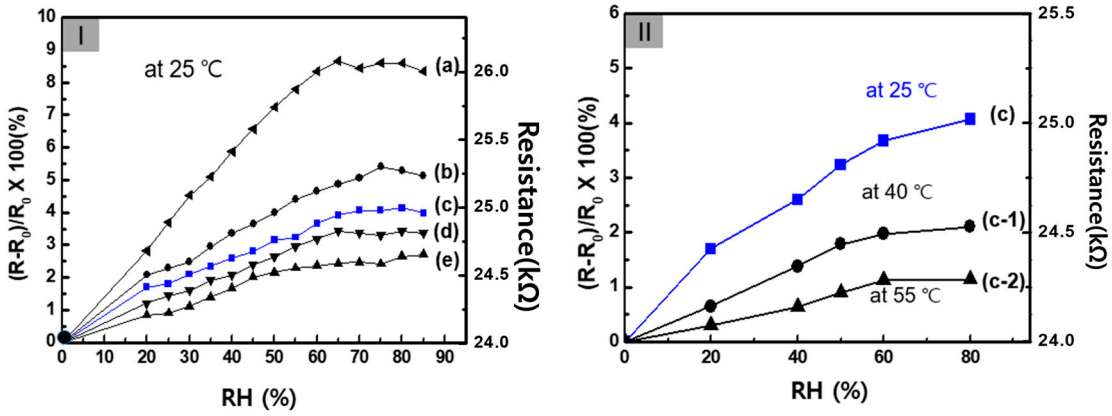

Figure 4. (I) Sensor response of SWCNT/C4F-PPy film exposed to different humidity conditions at 25 ℃; the mole ratio of C4F is (a) 0, (b) 0.05, (c) 0.1, (d) 0.2, and (e) 0.3, respectively. (II) Electrical resistance of SWCNT/C4F-PPy sensor film with varying humidity at multiple temperature conditions; (c) 25 ℃

Preprints (www.preprints.org) | NOT PEER-REVIEWED | Posted: 7 July 2023 doi:10.20944/preprints202307.0467.v1

, (c-1) 40 ℃, (c-2) 55 ℃, respectively. The initial resistance (R_0) of the samples used in the experiment is 24 KΩ •cm.

We fabricated the gas sensor array by screen-printing a SWCNT/C4F-PPy nanocomposite ink solution onto the IDE substrate film (test cell: with a pair of integrated Cu/Ni/Au electrodes on a 50-μm-thick PI substrate), as shown in Figure 5. The surface morphology of the sensor layer made of one-dimensional SWCNT/C4F-PPy nanocomposite has a microporous structure in which a three-dimensional network appears to be entangled. It is known that PPy or SWCNT/PPy composite compounds show changes in electrical resistance according to typical characteristics of p-type semiconductors [27,28]. This is due to the charge transfer mechanism between the acetone molecule, which acts as an acid when exposed to acetone gas, and the positively charged polaron of the PPy backbone. Hence, the PPy interacts with acetone to gain an electron; this electron transfer between positively charged PPy and acetone causes an elevation in the charge-carrier concentration, which causes a decrease in the overall electrical resistance. In particular, the PLA molecule can more easily receive electrons from acetone, from which some of the hydroxyl groups are converted to OH_2^+, thereby increasing the positive charge density of the PPy backbone by self-doping. The sensor array film was placed in a gas chamber and the chamber was purged with pure dry air using a carrier gas for 10 min while maintaining the chamber at atmospheric pressure. Then, various concentrations of acetone gas were injected to the chamber under different temperature and humidity conditions. Electrical resistance (ohm/cm) was measured in real time using a digital multi-meter to record changes corresponding to different gas inflow. The sensor array films were used to detect acetone vapor and normalized the electrical-resistance change (defined as $\Delta R/R_0 \times 100$ ($\Delta R = R - R_0$), where R and R_0 are the real-time resistance and initial resistance, respectively) to evaluate response. When the sensor array film was exposed to pure acetone gas, then the electrical resistance increased rapidly and the response time was 750 s. Figure 5-(I) shows the response characteristics of the sensor array to injection of acetone gas in the range of 1 to 5 ppm. As shown in the figure, an response (S) was shown in the negative direction in each concentration condition, and the S tended to change proportionally as the gas concentration increased. However, as shown in Figure 5-(II), it was observed that S had a linear characteristic toward an increase in resistance as the concentration of injected gas increased. At this time, the sensitivity (ppm^{-1}) of the acetone gas sensor can be calculated as 0.37.

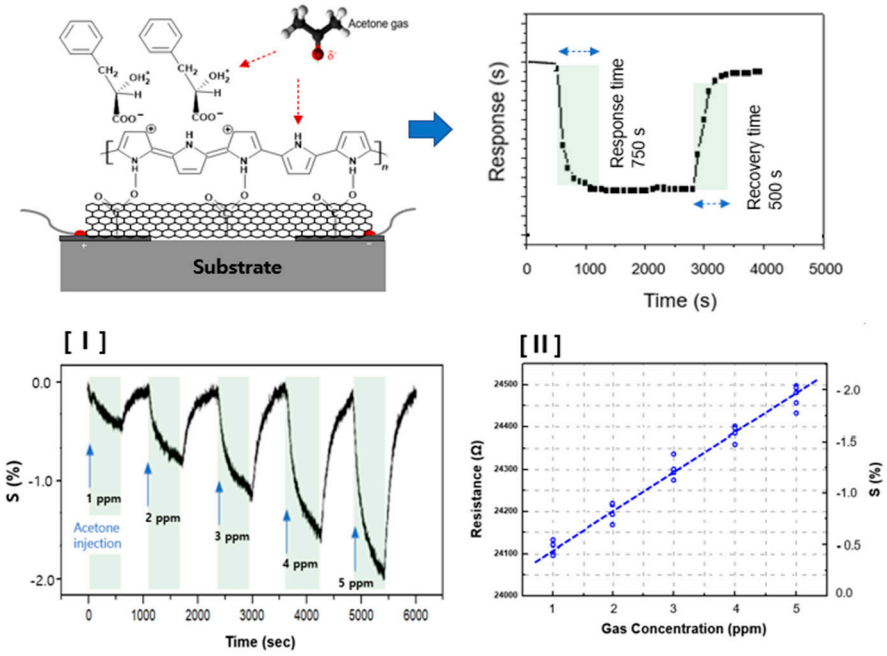

Figure 5. Schematic diagram of sensor array using SWCNT/C4F-PPy nanocomposite and dynamic response in sensors to various concentrations of acetone gas at 25 ℃ and 0% RH. Th resoinse (S) is

Preprints (www.preprints.org) | NOT PEER-REVIEWED | Posted: 7 July 2023 doi:10.20944/preprints202307.0467.v1

observed towards the negative direction as the gas is injected, which means that the sensor array resistance increases when the gas is injected. [I] The response spectrum of the SWCNT/C4F-PPy nanocomposite sensor to different concentrations of acetone gas as a function of time. [II] Change in response sensitivity according to the concentration of acetone gas from 1 to 5 ppm. The sensitivity (ppm^{-1}) of the acetone gas sensor can be calculated as 0.37.

Figure 6-(I-a) shows a representative data to illustrate the response characteristics of the sensor array film to acetone gas concentrations of 2.5 and 5 ppm at 25 ℃ and 0% RH. Acetone concentrations of 2.5 and 5 ppm resulted in response (S) measurements of 0.92 and 1.67, respectively, and the relative response time was slightly faster at the higher concentration. At 5 ppm of acetone vapor the S value of the sensor reached 1.67 within a response time of 750 s. For comparison purposes, Figure 6-(I-b) shows acetone response data of a sensor fabricated by drop-casting SWCNT/C4F-PPy nanocomposite ink solution onto Si substrate with an integrated Au electrode. Although the Cu/Ni/Au-based PI substrate sensor (Figure 6-(I-a)) demonstrates approximately a 5% difference in response from the Au-based Si wafer substrate sensor (Figure 6-(I-b)), the results show a similar level of response characteristics. Figure 6-(II-a) plots the measured change in sensor response under various humidity conditions when 5 ppm of acetone gas is injected to the chamber. As shown in Figure 6-(II), S showed a tendency to decrease rapidly when RH was 10% or more, and the change was generally linear. When RH was at the highest level of 80%, S decreased to 0.72. Compared to the Si wafer-based sensor (Figure 6-II-b), the PI-based film sensor (Figure 6-(II-a)) showed better response in the range of 10%–80% RH. Acetone gas was only weakly detected when RH was 80% or higher using the Si wafer-based sensor. These results indicate that the PI-based film sensor is better at sensing acetone gas in high humidity conditions.

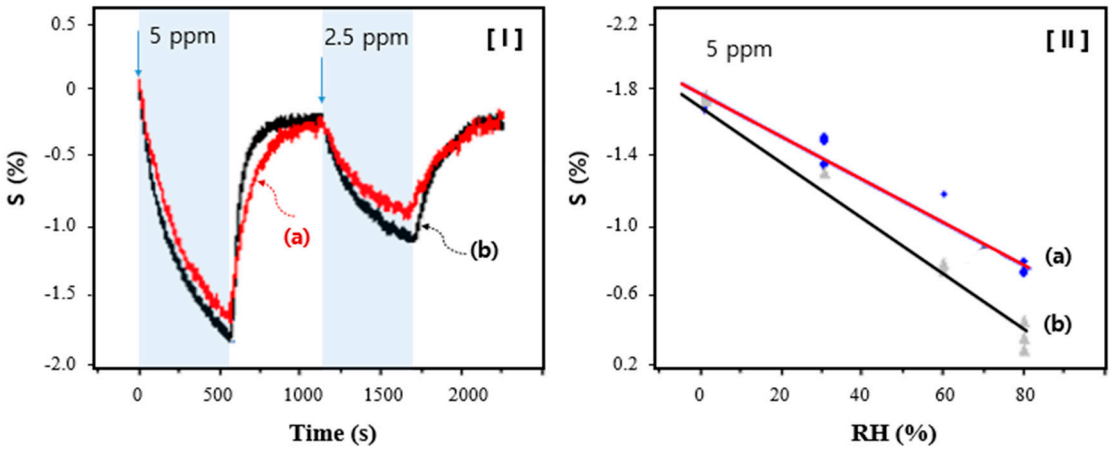

Figure 6. (I) The continuous dynamic response of the SWCNT/C4F-PPy nanocomposite sensor at different concentrations of acetone (2.5 and 5 ppm) at 25 °C/0% RH conditions. (II) Response changes with increasing humidity levels measured at 5 ppm acetone concentration under 25 °C. (a) PI film-based sensor integrated with Cu/Ni/Au electrodes, (b) Si wafer-based sensor integrated with Au electrodes. .

4. Conclusion

We synthesized a rod-shaped nanocomposite with SWCNT inserted into C4F-PPy by emulsion polymerization and used it as an acetone sensing material. SEM and TEM were used to analyze the structure of the nanorod-shaped SWCNT/C4F-PPy composite, and the contents of the constituent elements were confirmed from the EDS spectrum. A hybrid ink composition composed of SWCNT and C4F-PPy was directly coated on a flexible polyimide film interdigitated with the Cu/Ni/Au electrodes by a screen print process. This sensor film provided a response of 1.72% in 5 ppm of acetone, closely mirroring the sensor response characteristics of the Si wafer substrate. However, the sensor film performed better in high humidity conditions. In this study, the flexible type sensor film

synthesized in the low-temperature/continuous film process demonstrated the possibility for application across various fields.

Author Contributions: H.-K.K. and J.-H.B. participated in the experiment design, carried out the synthesis of materials, tested the films, and helped to draft the manuscript. H.-J.H. supported experimentation and data analysis. Y.-H. J. jointly conducted data interpretation and manuscript writing. J.-Y.K. wrote the paper and supervised the work as a project reader. All authors read and approved the final manuscript.

Funding: This work was financially supported by National Research Foundation of Korea (NRF) grant funded by the Korea government (Ministry of science and ICT: MIST) (2021R1F1A1105389111).

Conflicts of Interests: The authors declare that they have no known competing financial interests or personal relationships that could have appeared to influence the work reported in this paper. .

References

1. Tille, T. Automotive suitability of air quality gas sensor. *Sens. Actuators B* **2012**, *170*, 40–44.
2. Mohankumar, P.; Ajayan, J.; Yasodharan, R.; Devendran, P.; Sambasivam, R. A review of micromachined sensors for automotive applications. *Measurement* **2019**,*140*, 305–322.
3. Rydosz, A. Sensors for Enhanced Detection of Acetone as a Potential Tool for Noninvasive Diabetes Monitoring. *Sensors* **2018**, *18*, 2298.
4. Saidi, T.; Zaim, O.; Moufid, M.; Bari, N.E.; Ionescu, R.; Bouchikhi, B. Exhaled breath analysis using electronic nose and gas chromatography–mass spectrometry for non-invasive diagnosis of chronic kidney disease, diabetes mellitus and healthy subjects. *Sens. Actuators B* **2018**, *257*, 178–188.
5. Kita, J.; Schubert, F.; Retting, F.; Engelbrecht, A.; Gross, A.; Moos, R. Ceramic alumina substrates for high-temperature ga sensors-implications for applicatbility. *Proc. Eng.* **2017**, *87*, 1505–1508.
6. Rydosz, A.; Szkudlarek, A.; Ziabka, M.; Momanski, K.; Maziarz, W.; Pisarkiewicz, T. Performance of Si-Doped WO_3Thin Films for Acetone Sensing Prepared by Glancing Angle DC Magnetron Sputtering. *IEEE Sens. J.* **2016**, *16*, 1004–1012.
7. Ozdemir, S.; Gole, J.L. The potential of porous silicon gas sensors. *Curr. Opin. Solid State Mater. Sci.* **2007,** *11*, 92–100.
8. Lee, Y.M.; Zheng, M.R. Preparation of high-aspect-ratio ZnO nanorod arrays for the detection of several organic solvents at room working temperature, *Appl. Surf. Sci.*, **2013**, *285*, 241–248.
9. Xing, R.; Li, Q.; Xia, L.; Song, J.; Xu, L.; Zhang, J.; Xie, Y.; Song, H. Au-modified three-dimensional In_2O_3 inverse opals: synthesis and improved performance for acetone sensing toward diagnosis of diabetes, Nanoscale, **2015**, *7*, 13051–13060.
10. Khun, K.K.; Mahajan, A.; Bedi, R.K. SnO_2 thick films for room temperature gas sensing applications, *J. Appl. Phys.* **2009**, *106*, 124509.
11. Shi, J.; Hu, G.; Sun, Y.; Geng, M.; Wu, J.; Liu, Y.; Ge, M.; Tao, J.; Cao, M.; Dai, N. WO_3 nanocrystals: Synthesis and application in highly sensitive detection of acetone, *Sens. Actuators B*, **2011**, *156*, 820–824.
12. Liu, C.; Tai, H.; Zhang, P.; Yuan, Z.; Du, X.; Xie, G.; Jiang, Y. A high-performance flexible gas sensor based on self-assembled PANI-CeO_2 nanocomposite thin film for trace-level NH_3 detection at room temperature, *Sens. Actuators B* **2018**, *261*, 587–597.
13. Liu, B.; Liu, X.; Yuan, Z.; Jiang, Y.; Su, Y.; Ma, J.; Tai, H. A flexible NO_2 gas sensor based on polypyrrole/nitrogen-doped multiwall carbon nanotube operating at room temperature. *Sens. Actuators B*. **2019**, *295*, 86–92.
14. Zhou, X.; Guo, W.; Fu, J.; Zhu, Y.; Huang, Y.; Peng, P. Laser writing of Cu/CuxO integrated structure on flexible substrate for humidity sensing. *Appl. Surf. Sci*. **2019**, *494*, 684-690.
15. Kuberský, P.; Syrový, T.; Hamacek, A.; Nespurek, S.; Stejskal, J. Printed Flexible Gas Sensors based on Organic Materials. *Procedia Eng*. **2015**, *120*, 614–617.
16. Kumar, L.; Rawal, I.; Kaur, A.; Annapoorni, S. Flexible room temperature ammonia sensor based on polyaniline. *Sens. Actuators B*. **2017**, *240*, 408–416.
17. Cherenack, K.; Zysset, C.; Kinkeldei, T.; Munzenrieder, N.; Troster, G. Woven Electronic Fibers with Sensing and Display Functions for Smart Textiles. *Adv. Mater*. **2010**, *22*, 5178–5182.
18. Zhang, R.; Deng, H.; Valenca, R.; Jin, J.; Fu, Q.; Bilotti, E.; Peijs, T. Strain sensing behaviour of elastomeric composite films containing carbon nanotubes under cyclic loading. *Compos. Sci. Technol*. **2013**, *74*, 1–5.
19. Hua, C.; Shang, Y.; Wang, Y.; Xu, J.; Zhang, Y.; Li, X.; Cao, A. A flexible gas sensor based on single-walled carbon nanotube-Fe_2O_3 composite film. *Appl. Surf. Sci*. **2017**, *405*, 405–411.

20. Du, W.X.; Lee, H.J.; Byeon, J.H.; Kim, J.S.; Cho, K.S.; Kang, S.M.; Takada, M.; Kim, J.Y. Highly sensitive single-walled carbon nonotube/polypyrrole/phenylalanine core-shell nanorods for ammonia gas sensing. *J. Matter. Chem C.* **2020**, *8*, 15609–15615.
21. Cho, S.; Leel, J.S.; Jun, J.; Jang, J. High-sensitivity hydrogen gas sensors based on Pd-decorated nanoporous poly(aniline-co-aniline-2-sulfonic acid):pss, *J. Matter. Chem C.* **2014**, *2*, 1955–1966.
22. Byeon, J.H.; Kim, J.S.; Kang, H.K.; Kang, S.; Kim, J.Y. Acetone gas sensor based on SWCNT/polypyrrole/phenyllactic acid nanocomposite with high sensitivity and humidity stability, *Biosensors*, **2022**, 12, 354.
23. Liu, H.; Kameoka, J. D.; Czaplewski, A.; Craighead, H. G. Polymeric Nanowire Chemical Sensor. *Nano Lett*. **2004**, *4(4)*, 671–675
24. Li, X.; Zhang, W.; Wang, K.; Wei, J.; Wu, D.; Cao, A.; Li, Z.; Cheng, Y.; Zheng, Q. *Sci. Rep.* **2012**, *16*, 87
25. Liu, W.; Xu, L.; Sheng,K.; Zhou, X.; Dong, B.; Lu, G.; Song, H. *NPG Asia Matter*. **2018**, *10*, 293–308.
26. Kawashima, H.; Mayama, H.; Nakamura, Y.; Fujii, S. Hydrophobic polypyrroles synthesized by aqueous chemical oxidative polymerization and their use as light-responsive liquid marble stabilizers. *Polym. Chem.* **2017**, *8*, 2609–2618.
27. Hieu, N.; Dung, N.Q.; Tam, P.D.; Trung, T.; Chien, N.D. Thin film polypyrrole/SWCNTs nanocomposites-based NH_3 sensor operated at room temperature. *Sens. Actuators B*. **2009**, *140*, 500–507.
28. Jang, W.K.; Yun, J.M.; Kim, H.I.; Lee, Y.S. Improvement in ammonia gas sensing behavior by polypyrrole/multi-walled carbon nanotubes composites. *Carbon Lett*. **2012**, *13*, 88–93.